J|A|C|S
ARTICLES
Published on Web 12/22/2006

Modulation of Fluorescence through Coassembly of Molecules in Organic Nanostructures

Heather A. Behanna,[†] Kanya Rajangam,[‡] and Samuel I. Stupp[†,‡,§,*]

Contribution from the Department of Chemistry, Department of Materials Science and Engineering, Feinberg School of Medicine, Northwestern University, Evanston, Illinois 60208-3108

Received April 18, 2006; E-mail: s-stupp@northwestern.edu

Abstract: This paper describes the fluorescence of bimolecular coassemblies that form one-dimensional nanostructures. One molecule is a fluorescent peptide amphiphile containing its branched stilbene chromophore covalently linked to the hydrophilic end of the amphiphile, and the second molecule is a shorter, nonfluorescent peptide amphiphile of complementary charge. Using circular dichroism we observe that mixing both molecules results in coassemblies that exhibit a β-sheet signature in the peptide region indicative of these types of nanostructures. The nature of the coassembly is dependent on the molar ratio of each component, and the changing CD spectra suggest the formation of domains along the length of the nanofibers with decreasing concentrations of the fluorescent component. In coassemblies with dilute concentrations of the fluorophore, we observe an increase in fluorescence intensity and quantum yield, as well as chiral transfer to the achiral segment of the fluorescent peptide amphiphile. The coassemblies studied containing a fluorescent component at a low molar ratio exhibit fluorescence resonance energy transfer to fluorescent acceptors in solution. When the nonfluorescent peptide amphiphile component is designed to bind the important bioactive polysaccharide heparin, a selective transfer of energy is observed between fluorescein-tagged heparin and the coassemblies in both dilute solution and in macroscopic gels.

Introduction

The addition and covalent attachment of fluorophores to self-assembling systems has been used extensively in both materials and life sciences.[1−10] The most widely known example of this in biology is the use of the dye Congo Red to characterize the aggregation of peptides into β-amyloid structures, as the dye binds selectively to β-sheet fibrils and not to peptides in solution.[11,12] Another example is the use of fluorescent molecules that bind to self-assembling proteins of the cytoskeleton, such as tubulin.[13,14] Pyrene is a fluorophore that has been used to probe self-assembly due to its excimer emission that appears upon aggregation of the fluorophore.[15−18] This property of pyrene has been used as a tool to probe the conformation of aggregates,[15,19−22] or used in solution to study the encapsulation properties of aggregates.[16,23−25] Systems composed of both sodium dodecyl sulfate (SDS) and pyrene in differing ratios have also been used to create different sized nanostructures, each with varying optical properties.[18] Pyrene has also been used as a selective cation sensor when encapsulated in micelles.[26,27] Another fluorescent molecule in this field is azobenzene, which generally shows low fluorescence emission in solution, but recovers fluorescence upon aggregation into bilayers, spheres, and dendrimers.[28−34] Fluorescence has also been used to probe

[†] Department of Chemistry.
[‡] Department of Materials Science and Engineering.
[§] Feinberg School of Medicine.

(1) Ikeda, M.; Nobori, T.; Schmutz, M.; Lehn, J. M. *Chem.-Eur. J.* **2005**, *11* (2), 662.
(2) van Herrikhuyzen, J.; Syamakumari, A.; Schenning, A.; Meijer, E. W. *J. Am. Chem. Soc.* **2004**, *126* (32), 10021.
(3) Kumar, C. V.; Chaudhari, A. *Microporous Mesoporous Mater.* **2000**, *41* (1−3), 307.
(4) Balzani, V.; Credi, A.; Mattersteig, G.; Matthews, O. A.; Raymo, F. M.; Stoddart, J. F.; Venturi, M.; White, A. J. P.; Williams, D. J. *J. Org. Chem.* **2000**, *65* (7), 1924.
(5) Schillen, K.; Yekta, A.; Ni, S. R.; Farinha, J. P. S.; Winnik, M. A. *J. Phys. Chem. B* **1999**, *103* (43), 9090.
(6) Konig, B.; Pelka, M.; Zieg, H.; Ritter, T.; Bouas-Laurent, H.; Bonneau, R.; Desvergne, J. P. *J. Am. Chem. Soc.* **1999**, *121* (8), 1681.
(7) Chen, J. P.; Dabrowski, M. J.; Atkins, W. M. *Protein Eng.* **1997**, *10* (11), 1289.
(8) Visser, A. *Curr. Opin. Colloid Interface Sci.* **1997**, *2* (1), 27.
(9) Evans, C. E.; Bohn, P. W. *J. Am. Chem. Soc.* **1993**, *115* (8), 3306.
(10) Credi, A.; Balzani, V.; Langford, S. J.; Stoddart, J. F. *J. Am. Chem. Soc.* **1997**, *119* (11), 2679.
(11) Klunk, W. E.; R.F. J.; Mason, R. P. *Anal. Biochem.* **1999**, *266*, 66.
(12) Pigorsch, E.; Elhaddaoui, A.; Turrell, S. *J. Mol. Struct.* **1995**, *348*, 61.
(13) Andreu, J. M. *EMBO J.* **1982**, *1* (9), 1105.
(14) Sengupta, S.; Boge, T. C.; Georg, G. I.; Hiimes, R. H. *Biochem.* **1995**, *34*, 11889.
(15) Lindegaard, D.; Babu, B. R.; Wengel, J. *Nucleosides Nucleotides Nucleic Acids* **2005**, *24* (5−7), 679.
(16) Guler, M. O.; Claussen, R. C.; Stupp, S. I. *J. Mater. Chem.* **2005**, *15* (42), 4507.
(17) Tovar, J. D.; Claussen, R. C.; Stupp, S. I. *J. Am. Chem. Soc.* **2005**, *127* (20), 7337.
(18) Zhang, X.; Zhang, X.; Shi, W.; Meng, X.; Lee, C.; Lee, S. *J. Phys. Chem. B* **2005**, *109* (40), 18777.
(19) Cardona, C. M.; Wilkes, T.; Ong, W.; Kaifer, A. E.; McCarley, T. D.; Pandey, S.; Baker, G. A.; Kane, M. N.; Baker, S. N.; Bright, F. V. *J. Phys. Chem. B* **2002**, *106* (34), 8649.
(20) Barenholz, Y.; Cohen, T.; Haas, E.; Ottolenghi, M. *J. Biol. Chem.* **1996**, *271* (6), 3085.
(21) Pownall, H. J.; Smith, L. C. *Chem. Phys. Lipids* **1989**, *50* (3−4), 191.
(22) Winnik, F. M.; Winnik, M. A.; Tazuke, S.; Ober, C. K. *Macromol.* **1987**, *20* (1), 38.
(23) Lele, B. S.; Leroux, J. C. *Macromol.* **2002**, *35* (17), 6714.
(24) Liu, M. J.; Kono, K.; Frechet, J. M. J. *J. Controlled Release* **2000**, *65* (1−2), 121.
(25) Paleos, C. M.; Tsiourvas, D.; Sideratou, Z.; Tziveleka, L. *Biomacromolecules* **2004**, *5* (2), 524.
(26) Diaz Fernandez, Y.; Perez Gramatges, A.; Amendola, V.; Foti, F.; Mangano, C.; Pallavicini, P.; Patroni, S. *Chem. Commun.* **2004**, (14), 1650.
(27) Berton, M.; Mancin, F.; Stocchero, G.; Tecilla, P.; Tonellato, U. *Langmuir* **2001**, *17* (24), 7521.
(28) Han, M.; Hara, M. *J. Amer. Chem. Soc.* **2005**, *127*, 10951.

hydrogels, following the appearance of circular dichroism signal in the region of chromophore absorption upon gelation.[35] Materials such as quantum dots have also been used to transfer energy to protein−fluorophore acceptors via a fluorescence resonance energy transfer (FRET) mechanism.[36]

In our laboratory, we have studied the self-assembly of peptide amphiphiles (PAs) from aqueous solutions into nanofibers which in turn associate into networks that form gels.[17,37−42] Solvent accessibility to the interior of these nanofibers has been probed by fluorescence of both tryptophan and pyrene moieties covalently bound to the molecules.[16,17] These studies revealed solvent accessibility into the nanofibers, supporting a substructure of the nanofibers composed of β-sheets.

The accessibility of the periphery of aggregates opens up the possibility of using the nanofibers for biological sensing applications. Previous work in our laboratory has incorporated specific peptidic epitopes into the nanofibers to mimic binding sites on extracellular matrix proteins and promote cell adhesion or differentiation.[39,43,44] The interaction of biomolecules with these epitopes has been monitored indirectly by examining cell response[44] and directly by measuring binding constants between the PA and target molecules in dilute solution.[43,45] It is possible that the incorporation of a fluorescent moiety into the periphery of a peptide amphiphile could allow the formation of coassemblies to detect biomolecule−nanofiber interactions in dilute solution or in the gel state. Coassembly of two bioactive peptide amphiphiles of opposite charge has already been demonstrated by our laboratory,[39] as well as coassembly of epitope containing amphiphiles with non-bioactive ones.[40]

We report here the synthesis and characterization of a peptide amphiphile with a fluorophore on the hydrophilic end of the molecule. These molecules can be incorporated into coassemblies at varying molar ratios with nonfluorescent peptide amphiphiles to study the resultant effects of coassembly on both structure and fluorescence. We use circular dichroism in the ranges of both peptide and chromophore absorption to understand the coassembly of these molecules into one-dimensional nanostructures. Fluorescence emission of the coassemblies is also used to study the nature of the aggregation. Finally, we report on the use of these types of coassemblies to probe interactions with the biopolymer heparin. These initial studies suggest that these systems may be used to sense the presence of biomolecules or to study interactions of interest in biology.

Results and Discussion

In order to create supramolecular assemblies that can be tracked by fluorescence in biological systems, we first investigated if relatively large fluorescent peptide amphiphile (PA) molecules could interact with different nonfluorescent PAs described previously.[40] The objective was to create a generalizable approach to study phenomena using coassemblies of bioactive PAs and fluorescent ones which could in turn interact with external fluorophores in their environment.

Synthesis. We synthesized negatively charged and nonfluorescent **1** (containing 9 amino acid residues) and the fluorescent positively charged **2** (with 12 residues) based on the structure of **3** studied previously (see Chart 1).[40] **2** contains a hydrophilic fluorescent moiety that is soluble in neutral or basic water on its own and, as previously reported, is compatible with solid-phase synthesis.[46]

The synthesis of **2** utilized solid-phase chemistry using a Sieber resin modified with a fatty acid amino acid as has been described previously.[40] The Sieber resin was chosen because it is acid sensitive and the conditions for cleavage of the compound from the resin are compatible with the fluorophore. The amino acid sequence was the same as that in **3**, but a triple glycine spacer was added onto the amine terminus to enhance flexibility of the PA molecule and to extend the bulky fluorophore beyond the surface of the fiber when coassembled with other PA molecules. When peptide synthesis was complete, the fluorophore was added manually on solid phase by standard HBTU coupling procedures previously described.[46] The peptide conjugate was then cleaved from the resin and the protecting groups cleaved in solution to give **2** in 70% overall yield. The synthesis is described in detail in the experimental section.

PA Characterization. The secondary peptide structures in pure aggregates formed by PAs **1** and **2** were studied by circular dichroism, revealing the characteristic signature of a random coil for **1** as was previously reported,[40] and a β sheet signature for **2** (Figure 1). The CD spectrum for **3** shows a random coil signature, suggesting that the presence of the fluorophore in **2** leads to a β-sheet organization among its peptide segments. As a control, the PA with no fluorophore, but with the glycine spacer was synthesized, and this also gave a random coil signature by CD (data not shown). This suggests that the aromatic groups have an effect on molecular packing and that $\pi-\pi$ interactions may help align the positively charged segments of PA fibers. Upon dilution of **2** with water, the β-sheet signature decreases in amplitude and a more disordered signature appears with a minimum at 216 nm (data not shown).

The UV/vis absorption spectrum of **2** shows maxima corresponding to the fluorophore at 288 and 347 nm. **2** emits at 442 when excited at 345 nm, indicating no change in emission from the previously reported fluorophore without a peptide attached.[46]

Properties of Coassemblies. It was of interest to find out how the fluorescence would be affected as **2** coassembled with **1** in different molar ratios, with the intent of decreasing

(29) Jiang, W. H.; Wang, G. J.; He, Y. N.; An, Y. L.; Wang, X. G.; Song, Y. L.; Jiang, L. *Chem. J. Chinese Univ.* **2005**, *26* (7), 1360.
(30) Jiang, W. H.; Wang, G. J.; He, Y. N.; Wang, X. G.; An, Y. L.; Song, Y. L.; Jiang, L. *Chem. Commun.* **2005**, (28), 3550.
(31) Tsuda, K.; Dol, G. C.; Gensch, T.; Hofkens, J.; Latterini, L.; Weener, J. W.; Meijer, E. W.; De Schryver, F. C. *J. Am. Chem. Soc.* **2000**, *122* (14), 3445.
(32) Song, X. D.; Perlstein, J.; Whitten, D. G. *J. Phys. Chem. A* **1998**, *102* (28), 5440.
(33) Sano, M.; Sasaki, D. Y.; Isayama, M.; Kunitake, T. *Langmuir* **1992**, *8* (8), 1893.
(34) Shimomura, M.; Kunitake, T. *J. Am. Chem. Soc.* **1987**, *109* (17), 5175.
(35) Mahajan, S. S.; Paranji, R.; Mehta, R.; Lyon, R. P.; Atkins, W. M. *Bioconjugate Chem.* **2005**, *16* (4), 1019.
(36) Clapp, A. R.; Medintz, I. L.; Mauro, J. M.; Fisher, B. R.; Bawendi, M. G.; Mattoussi, H. *J. Am. Chem. Soc.* **2004**, *126* (1), 301.
(37) Hartgerink, J. D.; Beniash, E.; Stupp, S. I. *Science* **2001**, *294* (5547), 1684.
(38) Hartgerink, J. D.; Beniash, E.; Stupp, S. I. *Proc. Natl. Acad. Sci. U.S.A.* **2002**, *99* (8), 5133.
(39) Niece, K. L.; Hartgerink, J. D.; Donners, J.; Stupp, S. I. *J. Am. Chem. Soc.* **2003**, *125* (24), 7146.
(40) Behanna, H. A.; Donners, J.; Gordon, A. C.; Stupp, S. I. *J. Am. Chem. Soc.* **2005**, *127* (4), 1193.
(41) Bull, S. R.; Guler, M. O.; Bras, R. E.; Meade, T. J.; Stupp, S. I. *Nano Lett.* **2005**, *5* (1), 1.
(42) Arnold, M. S.; Guler, M. O.; Hersam, M. C.; Stupp, S. I. *Langmuir* **2005**, *21* (10), 4705.
(43) Guler, M. O.; Soukasene, S.; Hulvat, J. F.; Stupp, S. I. *Nano Lett.* **2005**, *5* (2), 249.
(44) Silva, G.; C, C.; Niece, K. L.; Beniash, E.; Harrington, D.; Kessler, J.; Stupp, S. I. *Science* **2004**, *303* (5662), 1352.
(45) Rajangam, K.; Behanna, H. A.; Hui, M. J.; Han, X.; Hulvat, J. F.; Lomasney, J. W.; Stupp, S. I. *Nano Lett.* **2006**, *6* (9), 2086.
(46) Behanna, H. A.; Stupp, S. I. *Chem. Commun.* **2005**, *38*, 4845.

Chart 1. List of PAs Synthesized

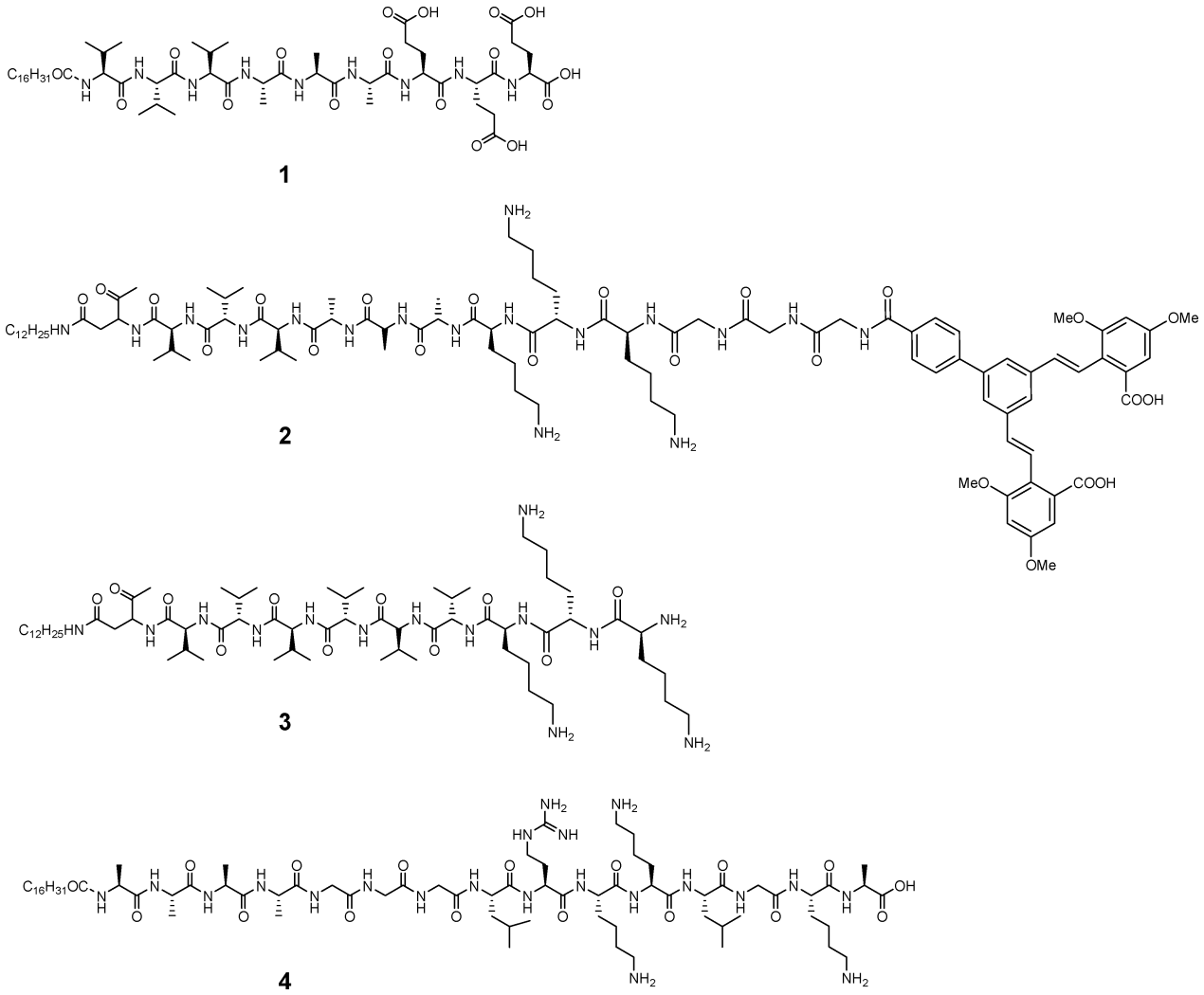

fluorophore concentration while maintaining the overall self-assembled nanostructures. A combination of CD in the peptide and fluorophore regions and fluorescence emission were used to study the resulting mixtures of molecules **1** and **2**. There were three main arrangements that could result from mixing (Figure 2). The first, called the "mixed coassembly" (Figure 2A) combines the two PAs homogeneously, as has been observed previously for systems without a fluorophore.[40] These types of aggregates would be expected to show a CD signature of a β-sheet that increases in amplitude with temperature as the addition of heat will allow for a more thermodynamically stable system that balances charge compensation with other short range forces. If the fluorophores are distributed as depicted in Figure 2A, an increase of fluorescence is expected as the fluorophores get diluted along the fiber, as has been observed in other micellar systems.[19,47,48] The second possibility, phase separated assembly (Figure 2B), would be the result of coassembly that gives rise to patches where one of the two PA molecules segregates instead of a homogeneously mixed system. For this scenario, the CD signature should reflect a linear combination of the spectra of **1** and **2**, and the fluorescence from **2** would not be expected to change as **1** was added. The third possibility is that both PAs do not coassemble at all (Figure 2C). These systems would be expected to show a linear combination of CD spectra in the peptide region and also should not exhibit a change in fluorescence compared to the assemblies of **2** alone.

Coassembly in Equal Molar Ratios. The first coassemblies investigated mixed **1** and **2** in equal molar amounts. The 1:1 mix shows a β-sheet signature, but the intensity of the signal is weaker than observed for **2** alone. This suggests that mixing of the oppositely charged structures disrupts the packing of the peptide segments of the nanofibers. At a 1:1 ratio, we also observe quenching of fluorescence for the aromatic part of the system, suggesting that $\pi-\pi$ stacking is even more prominent in the 1:1 mixture than in **2** alone, and in the UV spectrum one does not observe a change in the position of absorbance maxima compared to the spectrum of **2** alone, only an overall decrease in absorption (data not shown). To see if this packing arrangement was temperature dependent, variable temperature CD (VT−CD) was performed on the 1:1 mixture (see Supporting Information). As temperature increases, the β-sheet signal decreases linearly. We interpret this as evidence of aggregates being disrupted with rising temperature. Atomic force microscopy (AFM) performed on the 1:1 mixtures at room temperature and after heating shows that nanofibers do not form and only

(47) Sun, H.; Low, K. E.; Woo, S.; Noble, R. L.; Graham, R. J.; Connaughton, S. S.; Gee, M. A.; Lee, L. G. *Anal. Chem.* **2005**, *77*, 2043.
(48) Turchiello, R. F.; Lamy-Freund, M. T.; Hirata, I. Y.; Juliano, L.; Ito, A. S. *Biophys. Chem.* **1998**, *73* (3), 217.

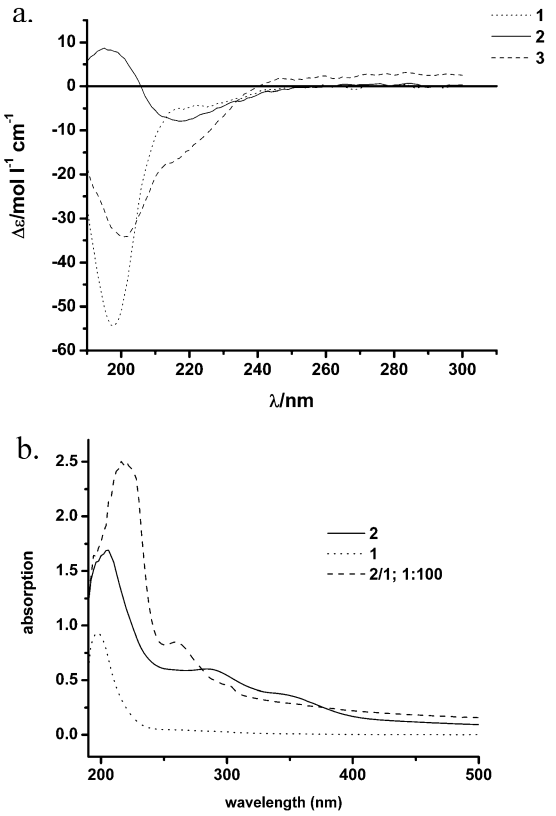

Figure 1. (a) CD spectra of **1** (black, dotted), **2** (black, solid), and **3** (black, dashed) in water at neutral pH. (b) UV spectra of PAs **2** and **1**, alone and mixed 1:100.

globular-like structures are observed (data not shown). It appears that the 1:1 packing in these systems is unfavorable, possibly due to the introduction of short range forces, namely $\pi-\pi$ stacking, that can disrupt hydrogen bonds, or due to the wedge shape of the fluorophore, a phenomenon observed in our laboratory with other fluorophore containing amphiphilic systems.[49]

Secondary Structure of Coassemblies of Varying Molar Ratios. In an attempt to create systems similar to those depicted by mixed coassembly (Figure 2A), further dilutions of **2** with **1** were attempted. After **2** is diluted with **1** at a ratio of 1:3, the β-sheet signature of the coassembly becomes stronger than **2** alone, suggesting that the mixtures have more perfectly aligned hydrogen-bonding structures. To further equilibrate these systems, the samples (beginning at dilutions of 1:3 (**2**/**1**)) were annealed at 37 °C overnight, as was done for model systems.[40] The CD spectra of the samples in the peptide region (190−300) were then recorded at room temperature.

The CD spectra of the annealed samples are shown in Figure 3. As **2** is diluted with **1** from 3 to 30 times, the β-sheet signal increases in intensity, suggesting an increase in the coherence length of perfectly aligned amide chromophores, potentially caused by the charge compensation of the oppositely charged PA molecules. This effect is maximized at a ratio of 1:250, beyond which an increasing random coil contribution is observed as more of **1** is added (see Figure 3). A linear combination of **2** and **1** cannot account for this behavior, suggesting there are other factors contributing to the new CD signature. These ratios contain a very large amount of **1**, which is by itself a random coil. Two possible packing modes can possibly explain the bimodal CD signature. One is that at these high dilution ratios, the assembly changes to a phase-separated coassembly as depicted in Figure 2B, exhibiting domains of pure **1** and domains of pure **2**. The other possibility is that mixed coassembly still exists (Figure 2A), but there are domains of pure **1** along with domains of mixtures of **2** and **1**. To further investigate this, both fluorescence and CD in the region of chromophore absorption was examined at varying dilutions of **2** with **1** in order to discriminate among various modes of mixing in the coassemblies.

Fluorescence of Coassemblies. For all fluorescence spectra, emission intensity was normalized for the amount of chromophore present. When **1** is present at up to 60 times the concentration of **2**, a quenching effect is observed compared to **2** alone, suggesting that in this dilution range the aromatic rings are stacked (see Supporting Information).[50] Beyond this dilution, an increase of intensity at 432 nm is observed, suggesting that at this point the fluorophores are more separated within the aggregates (Figure 4), supporting the existence of mixed coassembly as depicted in Figure 2A. These results can be replicated by dilution of **2** in water, suggesting that the increase of fluorescence is directly related to the aggregation of the fluorophores. This is supported by the UV absorption of the final ratio (**2**/**1**) of 1:100, where the peak at 347 nm is diminished, and the 288 nm peak shifts to 260 nm, suggesting that the chromophores are less aggregated in this diluted state. Quantum yields were also acquired for **2** alone and for **2** coassembled with **1**. It appears that the amphiphilic nature of the fluorophore has a significant effect on quantum yield, as the quantum yield for **2** is three times higher than the fluorophore without a peptide attached to it (0.038 versus 0.01).[46] The quantum yield for the diluted coassembly **2**/**1** (1:100) is 0.39. This substantial increase explains in part why such a large change in fluorescence emission intensity is observed in the diluted samples and may be due to the arrangement of the chromophores in space.

Evaluating the CD data in the context of the fluorescence data shows that a transition to a strong β-sheet signature in CD is observed at ratios where the fluorescence of the assemblies is quenched. Further, fluorescent intensity remains high when the CD spectrum exhibits a bimodal signature at a dilution of 1:500. This supports the proposed model of β-sheet-like domains with **2** distributed throughout the domains (mixed coassembly, Figure 2A), with other domains consisting purely of **1** with a random coil CD signature. If the PA molecules had become phase separated into regions of pure **1** and pure **2** (phase separated, Figure 2B), one would expect to see quenching of fluorescence as the fluorophores of **2** would be aligned as is observed for **2** alone.

CD Spectra of the Fluorophore. To further investigate the environment of the fluorophore in the highly diluted mixes, CD spectra were collected in the range of chromophore absorption at 260−350 nm. There is no chiral center present in the fluorophore segment of the molecule and **2** alone does not show a CD signal in the absorbance range of the fluorophore (see Figure 5). In supramolecular systems in the literature, it has been observed that chiral transfer can occur to an achiral

(49) Harrington, D. A.; Behanna, H. A.; Tew, G. N.; Claussen, R. C.; Stupp, S. I. *Chem. Biol.* **2005**, *12* (10), 1085.

(50) Li, X.; Xie, Y.; Chen, Z.; Zou, G. *Spectochim. Acta A* **2005**, *61*, 2468.

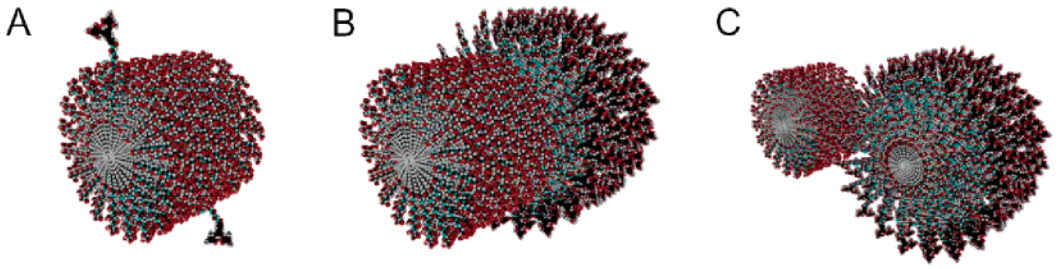

Figure 2. Possible outcomes of coassembly of PA **1** and PA **2**. Mixing of the two PA molecules can lead to three arrangements modeled above: (A) mixed coassembly (with 1 molecule of PA **2** for every 150 of PA **1**), (B) phase separated, and (C) not assembled, where there is no mixing at all.

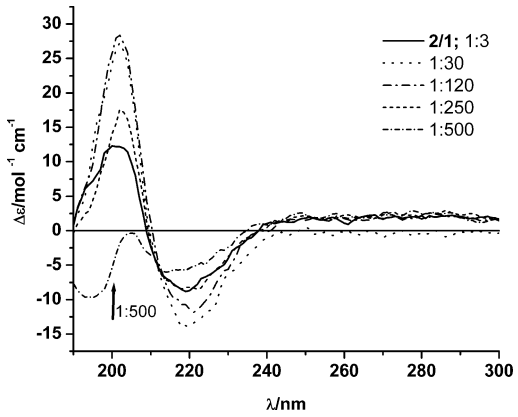

Figure 3. CD of the annealed **2**/**1** systems at different ratios.

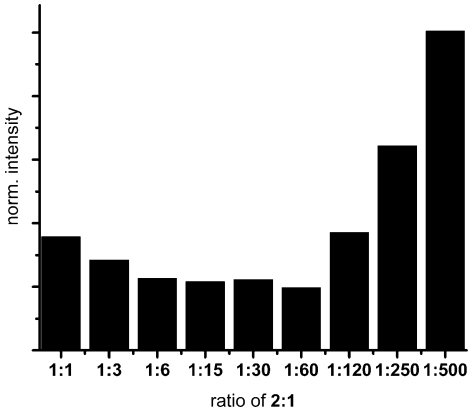

Figure 4. A graph of the intensity per fluorophore as **2** is mixed with increasing amounts of **1**. Intensity has been normalized to the concentration of the fluorophore. Intensity decreases until **2**/**1** 1:60 and then begins to increase.

component as a result of co-assembly.[51−55] For the coassembled **2**/**1** systems, a CD signal from the region of absorption of the fluorophore of **2** appears only at a ratio of **2**/**1** equal to 1:100. This signal (270 nm) persists at a dilution of 1:500 (see Figure 5), suggesting that the chromophore segments are not aggregated at these dilutions, supporting mixed coassembly (Figure 2A).

To examine further the structure of these assemblies, transmission electron microscopy was performed on a 1:120 dilution

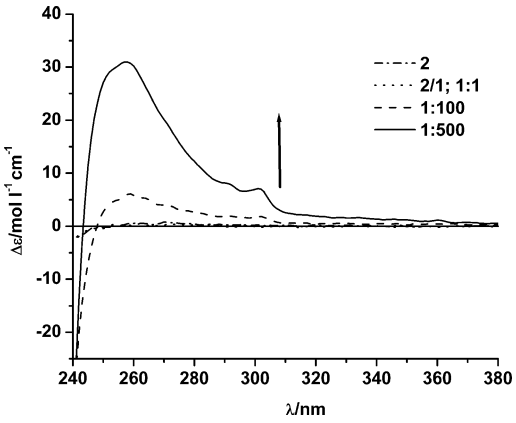

Figure 5. CD spectra in the absorption region of **2**. No signal is observed until the fluorophore is diluted 100-fold.

of **2** with **1** (see Supporting Information). These systems form fibers of dimensions consistent with other systems studied previously.[38−40] More in-depth study of the domain formation in these nanofibers is currently underway.

In summary, as the amount of **1** increases in the coassemblies, a β-sheet signature due to mixing of oppositely charged PAs is observed, but the aromatic rings of **2** are still in high enough concentration to be stacked and exhibit quenched fluorescence. As more of **1** is added, the molecules of **2** are separated within the nanofibers, leading to a recovery of fluorescence, and an arrangement similar to that depicted in Figure 2A. At very high dilutions (1:500, **2**/**1**), the domains surrounding the fluorophores become isolated by the large excess of **1**. A bimodal CD signature in the peptide region of the aggregates is observed, indicating the formation of domains consisting of only **1** in addition to mixed regions of PAs **1** and **2** (this is suggested by the random coil component of the CD signature). However, the two different molecules are still mixed, as demonstrated by a further increase in fluorescence and the presence of a CD signature in the region of chromophore absorption corresponding to **2**.

Fluorescent Sensing Applications. We were interested in using our fluorescent coassemblies to transfer energy to a biological acceptor via fluorescence resonance energy transfer (FRET) to monitor interactions between our materials and biomolecules of interest. FRET involves an excited state nonradiative energy transfer between a donor and acceptor chromophore and has been used previously to monitor interactions through space in cellular systems.[56−67] This energy transfer varies strongly with distance ($\sim 1/r^6$), making it a very powerful technique for imaging specific interactions between two macromolecules.[68−70]

(51) Fasel, R.; Parschau, M.; Ernst, K.-H. *Angew. Chem., Int. Ed.* **2003**, *42* (42), 5178.
(52) Brunsveld, L.; Lohmeijer, B. G. G.; Vekemans, J. A. J. M.; Meijer, E. W. *Chem. Commun.* **2000**, (23), 2305.
(53) Mori, T.; Inoue, Y. *Angew. Chem., Int. Ed.* **2005**, *44*, 2582.
(54) De Feyter, S.; Grim, P. C. M.; Rucker, M.; Vanoppen, P.; Meiners, C.; Sieffert, M.; Valiyaveettil, S.; Mullen, K.; De Schryver, F. C. *Angew. Chem., Int. Ed.* **1998**, *37* (9), 1223.
(55) Avcibasi, N.; Smet, M.; Metten, B.; Dehaen, W.; De Schryver, F. C.; Bultynck, G.; Callewaert, G.; De Smedt, H.; Missiaen, L.; Boens, N. *Int. J. Photoenergy* **2004**, *6* (4), 159.

Using the data from **2**/**1** coassemblies as a guideline, it was determined that the best coassemblies between **2** and a nonfluorescent PA would be where **2** is diluted out between 100 and 200 times. This gives the most well-defined secondary structure of the aggregates in the peptide region, coupled with a nonaggregated fluorophore arrangement with high emissive efficiency. The nonfluorescent PA chosen (PA **4**) has an epitope that binds to heparin (Chart 1),[45] a large macromolecule that mediates binding of growth factors to different biological moieties. Heparin is available tagged with fluorescein, a chromophore whose absorption matches the emission of **2**, making it ideal for this study. The epitope of this PA is a novel consensus sequence derived from the sequences of many heparin binding proteins present in nature.[71] PAs **2** and **4** were mixed in a ratio of 1:150 and then annealed overnight in solution. Evidence of coassembly was observed by CD (data not shown) and by macroscopic measures, as discussed below. A control mixture of PAs **2** and **1** was prepared under the same conditions. Both of the coassembled PA nanofibers were then placed in dilute solution, fluorescent heparin was added, and the spectral change monitored when exciting at 300 nm, a wavelength that shows minimal fluorescein emission (data not shown). For the **2**/**4** coassemblies, as heparin was titrated in, the emission of **2** decreases and the emission of fluorescein increases (see Supporting Information). The large increase observed in fluorescein emission at 513 nm suggests that the heparin is bound to the PA aggregate, close to a molecule of **2**. The **2**/**1** coassembly was then studied in the same manner to see if the energy transfer was a result of specific or nonspecific binding. As heparin was titrated into the solution, the emission of fluorescein increases slightly; however, the levels are close to background and much less intense than observed for the system where the heparin binder is present (see Supporting Information). To directly compare the system with a binding component (**2**/**4**) to one without (**2**/**1**), the ratio of intensity between the donor and acceptor in both systems was plotted (see Figure 6). These data strongly suggest that the energy transfer observed in these systems is due to the presence of the heparin binding **4** and not a more general association or entanglement with the aggregates.

Once FRET experiments were carried out in dilute solution, the energy transfer was examined in a gel formed by the fibers to establish with the relevance of these systems to microscopy to later monitor events *in vitro*, in real time. Gels were prepared of **2**/**4** and **2**/**1** in a ratio of 1:150 and annealed. The gels were then suspended in dilute solution, and the suspensions were

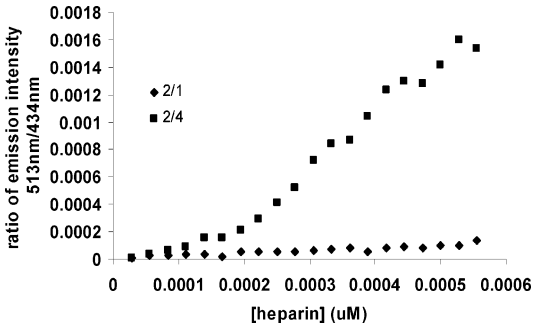

Figure 6. The ratio of intensity between the acceptor emission and donor emission as more heparin−fluorescein is added to the solution. When the heparin binder is present, there is a much larger increase in fluorescein emission.

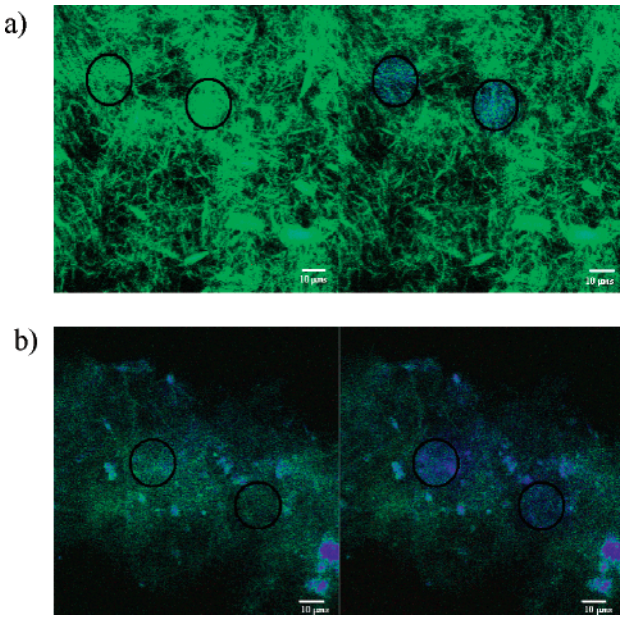

Figure 7. Photobleaching experiments. (a) Bundles of **2**/**4** coassemblies pre- (left) and post-photobleaching (right). The blue shows emission of **2**, the donor, and the green shows emission of fluorescein, the acceptor attached to heparin. When the area in the black circle is bleached, a recovery of the donor emission is observed. (b) Same experiment conducted for the control **2**/**1** system. The prebleach image shows some emission from the donor (blue), implying insufficient transfer of energy to the acceptor to give rise to acceptor emission (green).

examined by confocal microscopy in the presence and absence of fluorescent heparin. To establish that the fluorescence changes observed when heparin is added are due to FRET, acceptor photobleaching experiments were conducted, as recovery of donor emission only occurs with FRET.[58,66,72] In these experiments, a portion of the gel was compared both before and after photobleaching to monitor recovery of donor fluorescence. A small area of the fibers was saturated with light to bleach the fluorescein acceptor, and this area was imaged both before and after photobleaching. If FRET occurs, bleaching of the acceptor will allow for recovery of emission from the donor. This is in fact what we observed, as shown in Figure 7.

The same experiment was conducted for the control **2**/**1** gels, but even in the prebleaching image, some emission is seen from the donor, background that is not observed for the **2**/**4** gels (see Figure 7). When the photobleaching experiments are conducted,

(56) Evellin, S.; Mongillo, M.; Terrin, A.; Lissandron, V.; Zaccolo, M. *Methods Mol. Biol.* **2004**, *284*, (Signal Transduction Protocols (2nd ed.)), 259.
(57) Kikuchi, K.; Takakusa, H.; Nagano, T. *Trends Anal. Chem.* **2004**, *23* (6), 407.
(58) Burack, W. R.; Shaw, A. S. *J. Biol. Chem.* **2005**, *280* (5), 3832.
(59) dos Remedios, C. G.; Moens, P. D. *J. Struct. Biol.* **1995**, *115* (2), 175.
(60) Johnson, A. E. *FEBS Lett.* **2005**, *579* (4), 916.
(61) Lankiewicz, L.; Malicka, J.; Wiczk, W. *Acta Biochim. Polonica* **1997**, *44* (3), 477.
(62) *62. Matyus, L. J. Photochem. Photobiol. B* **1992**, *12* (4), 323.
(63) Muntau Ania, C.; Roscher Adelbert, A.; Kunau Wolf, H.; Dodt, G. *Eur. J. Cell. Biol.* **2003**, *82* (7), 333.
(64) Pollok, B. A.; Heim, R. *Trends Cell Biol.* **1999**, *9* (2), 57.
(65) Parsons, M.; Vojnovic, B.; Ameer-Beg, S. *Biochem. Soc. Trans.* **2004**, *32* (3), 431.
(66) Szabo, G., Jr.; Pine, P. S.; Weaver, J. L.; Kasari, M.; Aszalos, A. *Biophys. J.* **1992**, *61* (3), 661.
(67) Zal, T.; Gascoigne, N. R. J. *Curr. Opin. Immunol.* **2004**, *16* (5), 674.
(68) Hink, M. A.; Bisseling, T.; Visser, A. *Plant Mol. Biol.* **2002**, *50* (6), 871.
(69) Berney, C.; Danuser, G. *Biophys. J.* **2003**, *84* (6), 3992.
(70) Medintz, I. L.; Clapp, A. R.; Mattoussi, H.; Goldman, E. R.; Fisher, B.; Mauro, J. M. *Nature Mat.* **2003**, *2* (9), 630.
(71) Cardin, A.; HJ., W. *Arteriosclerosis* **1989**, *9* (1), 21.
(72) Snippe, M.; Borst, J. W.; Goldbach, R.; Kormelink, R. *J. Virol. Methods* **2005**, *125* (1), 15.

the donor does not recover as completely as for the **2**/**4** system. A ratio of the change in donor emission both before and after photobleaching to obtain FRET efficiency was calculated and plotted, showing the statistically significant ($p < 0.5$) difference between the **2**/**4** (0.79) and the **2**/**1** (0.63) systems (see Supporting Information). Although the **2**/**1** coassembled gels show some FRET efficiency, the data indicate a more intense energy transfer in the coassemblies designed to bind heparin.

Conclusions

We have demonstrated that coassembly of peptide amphiphiles (PA) is a powerful way to modify the fluorescence intensity of chromophores on the periphery of nanofibers. The CD data suggest strong coassembly at varying ratios and show a possible appearance of microdomains along the length of the nanofibers. Fluorescence intensity can be tuned in these supramolecular coassemblies for their efficient use as donors in energy transfer. Since protein epitopes can be easily incorporated in these nanostructures, they could be useful in studying the interactions of materials with proteins and also in the design of bioactive materials.

Experimental Section

General. All resins and Fmoc-L-amino acids were obtained from Novabiochem (San Diego, CA). All reagents for solid-phase synthesis were of synthesis grade and obtained from Applied Biosystems (Foster City, CA). All other reagents were obtained from Aldrich Chemical Co. (Milwaukee, WI) and used as received. Solvents for solid-phase peptide synthesis were acquired from Applied Biosystems and were peptide synthesis grade. Other solvents were obtained from Fisher Scientific and were used as received unless stated otherwise.

Peptide amphiphiles were synthesized using an Applied Biosystems 433A automated peptide synthesizer. NMR spectra were acquired on a Varian Inova 500 MHz spectrometer at room temperature. Electrospray ionization mass spectra were collected on a Micromass Quattro II triple quadrupole HPLC/MS/MS mass spectrometer. HPLC traces were obtained on a Rainin Instruments HPLC on commercially available reverse phase column (C18). Eluents (A): 0.1% formic acid in water and (B): 80% acetonitrile/water containing 0.08% formic acid was used in a gradient of 100/0 to 0/100 A/B over 22 min at a flow rate of 1.5 mL/min. The HPLC traces were tracked by UV absorption at 260 nm.

CD spectra were recorded on a Jasco J-715 spectropolarimeter with a Jasco PTC-348WI peltier-effect temperature controller. For CD experiments in the 260−400 nm range, the samples were made more concentrated, so that the UV−vis absorption at 260−300 nm was about 1. At these concentrations, the amide absorbance was over 2, too high for CD measurements. Fluorescence emission and excitation spectra were conducted on an ISS PC1 photon counting steady-state fluorescence spectrometer equipped with a 300 W xenon arc lamp. Slit widths of 2 mm (16 nm bandwidth) were used, and the xenon lamp power supply was set to 18 A. Excitation and emission wavelengths were set as stated in the text. All samples were run at a concentration where the absorption of the chromophore was not greater than 0.2 (micromolar concentrations). Quantum yield experiments were conducted in acidic water using quinine sulfate ($\phi = 0.546$) as a standard.

For the FRET experiments, PA molecules were annealed overnight with the donor fluorophore peptide amphiphile molecules (molar ratio **4**:**2** 150:1), and 0.5 w/ v % gels were made using disodium hydrogen phosphate solution. The images of the photobleaching experiments were captured using the specific FRET Zeiss software to monitor recovery of donor fluorescence. Specifically, in this case, the sample was excited at 405 nm and 20 images were captured between wavelengths of 422 to 636 nm (stepsize of 11 nm). A small area of the fibers was saturated with light at 488 nm, within the absorption band of fluorescein, effectively bleaching the acceptor for the FRET system. The same area was then imaged as done before the bleaching. If there is a specific FRET response occurring, the bleaching of the acceptor will allow for fluorescence of the donor. FRET efficiency was calculated as previously published after normalizing for bleaching due to imaging using the formula, efficiency = 1− (peak prebleach donor emission/peak postbleach donor emission).[69] In this case donor emission at 470 nm, which was its peak emission wavelength, was used to calculate the FRET efficiency ($n = 4 - 6$, t test assuming samples of unequal variance gave a p value of 0.02 comparing the heparin binding PA system with the control).

PA Synthesis and Purification. PAs **1**, **3**, and **4** were prepared as described in ref 18. For **2**, the standard Sieber resin was modified, as has been reported,[40] and then loaded onto the automated synthesizer, and peptide synthesis proceeded as for PAs **1**, **3**, and **4**. The PA was then removed from the synthesizer and placed into a vessel for manual attachment of the fluorophore as described previously.[46] Once coupling was complete, the PA was cleaved from the resin with 3% TFA in methylene chloride for 15 min. The solvent was then evaporated *in vacuo*, and ether was added until the PA precipitated. The PA was then collected and placed in a mixture of THF and water and deprotected with lithium hydroxide for 3 h.[46] The reaction was quenched with HCl, and the THF was evaporated *in vacuo*, causing the product to precipitate out. The compound was pure by HPLC and was then placed in anhydrous HCl in dioxanes overnight to deprotect the lysine residues. The solution was evaporated *in vacuo*, affording the pure product **2**.

Data for Asp(CONHC12)-Val-Val-Val-Ala-Ala-Ala-Lys-Lys-Lys-Gly-Gly-Gly fluorophore (**2**). ^{1}H NMR (d_6-DMSO): 7.67 (br s, 2H), 7.61 (br s, 4H), 7.56 (br s, 3H), 7.47 (br s, 2H), 7.42 (br s, 5H), 7.36 (br s, 3H), 7.27 (br s, 6H), 3.94 − 4.16 (m, 15H, C_α), 3.95 (m, 12H, $ArOCH_3$), 3.6 − 3.8 (m, 6H, Lys H_ϵ), 2.68 (s, 2H, tail CH_2NH), 2.15 (m, 6H, Val H_β), 2.07 (s, 6H, Lys H_δ), 1.88 (m, 12H, Lys $H_\beta + H_\gamma$), 1.22 (br s, 20H, tail C_{10}), 1.15 (br s, 9H, Ala H_β), 1.02 (m, 3H, tail CH_3), 0.84 (br s, 18H, Val H_γ). ESI MS (MeOH/H_2O, 1:1 v/v) expected: 1958.3 (MH^+), found 979.1 ($MH^+/2$).

Acknowledgment. This work made use of the Keck Biophysics Facility and the Analytical Services Laboratory at Northwestern University. The work was supported by the U.S. Department of Energy (DE-FG02-00ER54810) and the National Institutes of Health (NIH) (R01 EB003806-01). The authors would like to thank Rafael Bras and Liang-Shi Ling for their contributions of AFM and TEM imaging.

Supporting Information Available: Additional CD spectra, fluorescence spectra, and microscopy of peptide amphiphile coassemblies. This material is available free of charge via the Internet at http://pubs.acs.org.

JA062415B